Improved Topical Antifungal Medication using Sertaconazole Bilosomes: *In vitro* Permeability, Cytotoxicity, and Clinical Assessment

Omar Magdy Eldemiri [a*], Germeen NS Girgis [a], Sara Hamdy Fouad [b] and Thanaa Mohamed Borg [a]

[a] *Department of Pharmaceutics, Faculty of Pharmacy, Mansoura University, Mansoura 35516, Egypt.*
[b] *Department of Dermatology, Andrology and STDs, Faculty of Medicine, Mansoura University, Mansoura 35516, Egypt.*

Authors' contributions

This work was carried out in collaboration among all authors. Author OME did the methodology, software, validation, data curation, writing and original draft. Authors GNSG and SHF did the study conceptualization, visualization, investigation, validation, data curation, supervision, writing, review and editing. Author TMB did the conceptualization, visualization, investigation, validation, supervision, writing, review and editing. All authors read and approved the final manuscript.

Original Research Article

ABSTRACT

Objective: The purpose of the current study was to develop Sertaconazole bilosomes (SBs) with enhanced permeability, skin deposition, anti-fungal properties, and clinical efficacy.
Methods: By changing span 60 to cholesterol molar ratio, bile salt type, and concentration, 12 formulations of SBs were prepared using the thin film hydration method and characterized by particle size (PS), zeta potential (ZP), polydispersity index (PDI), % entrapment efficiency (% EE),

_____

*Corresponding author: E-mail: omarmagdi@mans.edu.eg.com;

and % cumulative drug released after 8h (% Q_{8h}) and 24h (% Q_{24h}). The optimized formulation (SB 5) was incorporated into 1% Carbopol 940 hydrogel (SBG 5) and tested for ex-vivo permeability, skin deposition, and anti-fungal efficacy compared to the commercial formulation (Dermofix® cream) and sertaconazole alone hydrogel (SAG). A randomized controlled clinical trial of SBG 5 compared to Dermofix® cream and SAG was done on 30 patients diagnosed with *Tinea corporis* with a 4-week follow-up.

Results: SB 5 showed PS of 158 ± 6.4nm, ZP of −55 ± 1.7mV, PDI of 0.16 ± 0.01, % EE of 96 ± 3.4, % Q_{8h} of 70.3 ± 3.6, and % Q_{24h} of 97.2 ± 3.0. SBG 5 exhibited in vitro release after 24h (1.25 and 1.51-fold), skin permeability (1.6 and 2.3-fold), skin deposition (3.86 and 14.82-fold), and anti-fungal efficacy against *Candida albicans* (two and 1.44-fold) compared to Dermofix® cream and SAG respectively. Patients receiving SBG 5 exhibited a 1.25 and 1.8-fold higher recovery rate on days 14 and 21 respectively compared to Dermofix® cream, and a 4.5 and two-fold recovery rate on days 14 and 21 respectively compared to SAG.

Conclusion: Bilosomes could be utilized to enhance permeability, skin deposition, anti-fungal properties, and clinical efficacy of Sertaconazole.

1. INTRODUCTION

Regarded as one of the most common skin conditions, superficial fungal infection affects 25% of people globally [1,2]. The growing number of immunocompromised individuals and the extensive use of swimming pool facilities are major contributing factors to the dramatic rise in infection incidence [3-5]. Dermatophytes being part of the Epidermophyton, Microsporum, and Trichophyton genera are the most common cause of superficial fungal infections. Additionally, yeasts and non-dermatophyte molds could produce similar lesions [6,7]. These infections are mainly observed in the superficial stratum corneum of the epidermis and its keratin-rich appendages such as the hair and nails. The effectiveness of a particular antimycotic drug in eliminating fungal isolates determines the course of treatment [8-10].

Sertaconazole (STZ) is a broad-spectrum imidazole antifungal that acts effectively against most fungi that cause superficial cutaneous infections such as yeasts and dermatophytes [11-13]. STZ, like other azoles, has two modes of action, fungistatic and fungicidal [13-15]. STZ selectively inhibits ergosterol biosynthesis, which causes a decrease in the cell membrane integrity followed by a disruption of normal cell growth and replication [12,13,16,17]. Moreover, at higher concentrations, STZ directly binds to non-sterol lipids in the fungal membrane altering its permeability, resulting in leakage of intracellular components and cell death as a consequence [12,16,18,19]. Unlike other azoles, STZ has excellent safety with low incidence of side effects [20-22]. Being hydrophobic, STZ shows limited water solubility leading to poor skin penetration [23-25]. So, different attempts have been used to either localize STZ in the layers of the skin or enhance its penetration and absorption through the skin such as cyclodextrin complexation [23] and incorporation into mixed micelles [26], microemulsions [27], and nanofibers [28].

Developing innovative drug delivery systems that can get around the problems with traditional systems is crucial because of the rise in fungal infections and resistance to antifungal drugs delivered by conventional systems [29]. In recent years, bilosomes have been identified as possible delivery systems for better topical, transdermal, ophthalmic, and oral administration of medications and vaccines. Bilosomes are closed bilayer vesicles consisting of non-ionic amphiphiles, the same as niosomes but incorporating bile salts. The primary distinction between bilosomes and niosomes is thought to be the nature of the vesicular wall; niosome structure does not include the extra edge activators (EAs) of bile salts [30-36]. Bile salts could be introduced into the lipophilic mixture directly and then dissolved in the organic solvent during the thin film formation step, or introduced with the aqueous medium during the thin film hydration step into the thin film formed after organic solvent evaporation [37]. By lowering surface tension, EAs cause the vesicular bilayer to become unstable, resulting in the formation of deformable vesicles with improved tissue penetration. As a result, the addition of bile salts improves the stability of the colloidal system, particle size diameter, and the fluidizing effect, which enhances drug permeability and deposition in the skin [38-42].

To the best of our knowledge, STZ-loaded bilosomes (SBs) have not been investigated to date. So, this work aimed to formulate SBs to enhance in vitro release, permeability, skin deposition, anti-fungal properties, and the clinical efficacy of STZ. Different SBs were prepared, evaluated, and optimized. The optimized formulation was incorporated into a hydrogel and tested for ex-vivo permeability, skin deposition, anti-fungal properties, and clinical efficacy.

2. MATERIALS AND METHODS

2.1 Materials

Sertaconazole nitrate (STZ) was generously provided by E.G.P.I. (Egyptian group for pharmaceutical industries) company, Egypt. Sodium deoxycholate (SDC) was obtained from Acros Organics, Belgium. Sodium dehydrocholate (DE) was obtained from European Egyptian Pharmaceuticals, Egypt. Span 60 (SP 60) was received from Qualikems, India. Cholesterol (CH) was obtained from ADVENT, India. Carbopol 940, triethanolamine (TEA) and methylparaben were obtained from LANXESS, Germany. Cellulose membrane (molecular weight cut-off 12,000–14,000) was purchased from Sigma Chemical Company (USA). HPLC grade methanol, ethanol, and chloroform were purchased from Fisher Scientific Co., UK. Nylon millipore syringe filter, 0.45 μm, Berlin, Germany. Disodium hydrogen phosphate, potassium hydroxide, and potassium dihydrogen phosphate were purchased from El-Nasr Pharmaceutical Co. (Cairo, Egypt).

2.2 Preparation of Sertaconazole Bilosomes by the thin Film Hydration Method

The thin film hydration method was used to prepare 12 formulations of Sertaconazole bilosomes (SBs) [32,43]. The composition of SBs is presented in Table 1. Briefly, bile salt (40 or 20 μmol), STZ (20 mg), and lipid mixture (210 or 230 μmol of SP 60 and CH taken in 2:1, 1:1, and 1:2 molar ratios) were dissolved in 10 ml organic solvent of a chloroform and methanol mixture (7:3). The resultant clear solution was removed to form a thin dry film by slow evaporation under reduced pressure for 30 min at 60 °C and 90 rpm using a rotary evaporator (Rotavapor, Heidolph VV 2000, Burladingen, Germany). The resultant dry film was then hydrated with 10 ml phosphate buffer (pH = 7.4) under normal pressure for 30 min at 60 °C and 150 rpm using the same apparatus, followed by a 30-minute bath sonication (Ultrasonic bath sonicator, Model Sonix IV SS101H 230; USA) at 25 °C to obtain SBs suspension containing both free and entrapped drug.

2.3 In vitro Characterization of Sertaconazole Loaded Bilosomes

2.3.1 Determination of the particle size, polydispersity index and zeta potential

The average particle size (PS) and polydispersity index (PDI) of all formulations were determined by Photon Correlation Spectroscopy (PCS) using a Zetasizer nano-ZS (Malvern Instrument, UK). The formulations were suitably diluted with distilled water and the analysis was performed at 25 °C and 173° angle of detection using the helium-neon laser of 633 nm in disposable clear cells. The size distribution's width was measured using the PDI. A homogeneous and monodisperse population is indicated by a PDI of less than 0.4. Zeta potential (ZP) measurement was also carried out at 25 °C by the same instrument using the laser Doppler velocimetry function [32,44].

2.3.2 Determination of entrapment efficiency (% EE)

The suspensions of SBs were centrifuged using a cooling centrifuge (Sigma 3K 30, Germany) at 13,000 rpm for two hours at 4 °C. After centrifugation, the resultant sediments were lysed with methanol and analyzed for STZ at 260 nm using a UV-Vis spectrophotometer (Shimadzu UV 1650 Spectrophotometer, Japan) against blanked bilosomes. Triplicate runs of each experiment were conducted. Equation (1) was utilized to calculate % EE [45].

$$\% \text{ EE} = \left(\frac{\text{ES}}{\text{TS}}\right) \times 100 \tag{1}$$

Where % EE is the entrapment efficiency percent, ES is the amount of entrapped STZ and TS is the total STZ content.

2.3.3 In vitro drug release

To investigate STZ release from freshly prepared SBs, modified Franz diffusion cells with an effective diffusion area of 3.8 cm^2 were utilized [28,46]. In a shaking incubator running at 100 rpm, a release medium (150 ml of 40% ethanol

to guarantee sink condition) was kept at 37±1ºC. A semipermeable cellulose membrane, equilibrated with the release medium for 24 hours, was firmly mounted between the donor and receptor compartments. In the donor compartment, each formulation was added, and at predetermined intervals of 0.5, 1, 2, 3, 4, 6, 8, and 24 hours, 5 mL aliquots of the release medium were withdrawn from the receptor compartment and replaced with an equal volume of fresh medium to preserve the sink condition during the whole experiment. At 260 nm, the obtained aliquots were analyzed for STZ using the UV–Vis spectrophotometer. Each experiment was done in triplicate and the percent cumulative STZ released was plotted versus time. Using zero-order, first-order, Higuchi matrix, Hixson-Crowell, and Korsmeyer-Peppas kinetic models, the STZ release mechanism was determined [28,47-53].

2.3.4 Transmission Electron Microscopy (TEM)

The optimized formulation (SB 5) morphology was examined by a transmission electron microscope (JEM-1230; JEOL, Tokyo, Japan) operating at 80 kV. After the dispersion was properly diluted with deionized water, a drop of the diluted dispersion was applied to a carbon-coated copper grid, stained with a 2% w/v solution of phosphotungstic acid, and then allowed to air dry for approximately five minutes before being examined by TEM [54].

2.3.5 Differential Scanning Calorimetry (DSC)

DSC analysis of STZ powder, SP 60, CH, SDC, the physical mixture of all components, and the optimized formulation (SB 5) was carried out with a differential scanning calorimeter (Shimadzu TA-60, Japan). The samples were precisely weighed (5 mg), packed airtightly in aluminum pans, and heated between 20 and 350 °C at a steady rate of 10 °C per minute. For reference, a sealed, empty aluminum pan was utilized. A 50 mL/min flow rate of dry nitrogen gas was employed as the carrier gas [26,55].

2.3.6 Fourier Transform Infrared spectroscopy (FT-IR)

FT-IR spectral studies in the range of 4000 and 500 cm^{-1} were performed on STZ powder, SP 60, CH, SDC, the physical mixture of all components, and the optimized formulation (SB 5) using an FT-IR spectrophotometer (Shimadzu IR-Affinity-1, Japan) to observe the chemical compatibility between STZ and the vesicle membrane components (SP 60, CH and SDC) [32].

2.3.7 Stability study

The stability of SB 5 was investigated for six months at ambient and refrigerated (4±1 °C) temperatures. Freshly prepared SB 5 suspensions were placed in glass vials, covered with aluminum foil, and kept at the above-mentioned temperatures. samples were withdrawn at definite time intervals (0, 1, 3, and 6 months) and analyzed for PS, % EE, PDI, and ZP as described earlier [32,56,57].

2.4 Hydrogel Preparation and Evaluation

Carbopol 940 was chosen as the macromolecular polymer gel matrix according to earlier studies for the preparation of the optimized formulation (SB 5) hydrogel (SBG 5) [58,59]. Briefly, one gram of Carbopol 940 was dispersed in an appropriate amount of water for 24 hours. SB 5 suspension (volume equivalent to 2% w/w of STZ in the final formulation) was slowly added to the highly viscous solution of Carbopol 940 under magnetic stirring. TEA was added dropwise till a semisolid gel-like consistency was obtained. With constant stirring, water was added to reach the final weight of 100 g of SBG 5 [60,61]. SBG 5 was evaluated for drug content, pH, and viscosity using a Brookfield cone and plate viscometer (LVDVIIPro Viscometer, Middleboro, MA) [27,32,62]. STZ alone hydrogel (SAG) was prepared with the same method except that pure STZ was used instead of SB 5.

2.4.1 *In vitro* drug release of SBG 5

The in vitro release of SBG 5, marketed product (Dermofix® cream), and STZ-alone hydrogel (SAG) were evaluated using the modified Franz diffusion cells by the method previously mentioned for the in vitro release of SBs [63].

2.4.2 Permeability and drug deposition study

2.4.2.1 Permeability study

Ex-vivo permeability study was performed for SBG 5, Dermofix® cream, and SAG on the skin obtained from ears of white albino rabbits using modified Franz diffusion cells having an effective diffusion area of 3.8 cm^2 [64]. Following hair

removal, the ear skin was carefully separated, washed with saline, and placed between the donor and recipient diffusion chambers at a constant temperature of 37 ± 0.5 °C in a shaking incubator running at 100 rpm. 5 ml aliquots of the recipient medium (100 ml of 40% methanol) were removed at pre-determined intervals of 0.5, 1, 2, 3, 4, 6, 8, and 24 hours, and promptly replaced with an equivalent volume of new recipient medium to preserve sink condition. After being filtered using a Millipore filter (0.45 μm), the collected aliquots were examined in the UV–Vis spectrophotometer at 260 nm against appropriate blanking. The cumulative amount of STZ that penetrated the skin was plotted as a function of time [60,65]. The study computed the parameters of STZ permeation through rabbit skin, including the cumulative amount of STZ permeated (D_n), the apparent permeability co-efficient (P_{app}), and the steady-state flux (J_{ss}) [66]. The cumulative amount of STZ permeated across the skin was determined using equation (2).

$$D_n = V_r C_{r(n)} + \sum_{x=1}^{x=n} V_{a(x-1)} C_{r(x-1)} \qquad (2)$$

where: n indicates sampling time point (n = 1, 2, 3…...10) corresponding to 0.5, 1, 2…...24 hours respectively); V_r and V_S represent the volume of the medium in the recipient chamber (100 mL) and the volume of the aliquot collected at the nth time point (5 mL); and $C_{r(n)}$ represents the concentration of the STZ in the recipient chamber at the nth time point (mg/mL). The rate of STZ permeated through the skin (dD/dt) was calculated from the slope of the cumulative amount of STZ permeated against time plot. The steady-state flux (J_{ss}) of STZ was computed according to equation (3):

$$J_{ss} = (dD/dt)/S \qquad (3)$$

where D and S represent the cumulative amount of STZ permeated and the surface area of the skin utilized in the experiment (3.8 cm^2). The apparent skin permeability co-efficient of STZ was calculated according to equation (4):

$$P_{app} = \frac{Flux\ (Jss)}{Cd} \qquad (4)$$

Where C_d represents the concentration of STZ in the donor chamber. The permeability enhancement ratio (ER) was computed according to equation (5):

$$ER = \frac{Jss\ (t)}{Jss\ (r)} \qquad (5)$$

Where Jss (t) and Jss (r) represent the steady-state flux of test and reference formulation respectively.

2.4.2.2 Drug deposition study

For the determination of STZ deposited in the skin, diffusion cells were disassembled after the 24-hour permeability study. Samples on the skin surface were carefully removed, and the skin was gently rinsed with water, chopped into little pieces, and homogenized with 50 ml of methanol for 24 hours under magnetic stirring for STZ to be extracted. Following a 30-minute, 10,000-rpm centrifugation of the homogenate dispersion, the supernatant was collected, filtered through a 0.45-micron membrane filter, and analyzed at 260 nm for STZ using a UV-visible spectrophotometer (UV-1800, Shimadzu) [65,67].

2.5 Microbiological Efficacy Assessment study

Using the agar well diffusion technique, the antifungal properties of SBG 5, Dermofix® cream, and SAG were assessed against *Candida albicans* derived from ATCC® 10231 (Ca), *Aspergillus brasiliensis* derived from ATCC® 16404 (Ab), and *Saccharomyces cerevisiae* derived from ATCC® 9763 (Sc). Sabouraud Dextrose Agar (SDA) plates were inoculated with the fungal suspension (10^4-10^5 CFU/ml). Next, using gel puncture, three 10-mm wells were made on each SDA plate. The wells were filled with one of the three formulations with the same STZ amount and then were incubated for 72 hours at 25 °C. Using a ruler, the diameters of the fungal growth inhibition zone were measured to determine the inhibition zones in mm. Each test was carried out three times [63,68].

2.6 *In vitro* Cytotoxicity

The in vitro cytotoxicity of SBG 5 formulation was evaluated by sulforhodamine B (SRB) colorimetric assay. Human skin fibroblast (HSF) cells were maintained in Dulbecco's Modified Eagle Medium (DMEM) media with 10% streptomycin, 100 units/ml of penicillin, and 10% heat-inactivated fetal bovine serum (HI FBS) supplementation, in a humidified atmosphere containing 5% CO_2 at 37 °C. 100 μL aliquots of the cell suspension, at a concentration of 5×10^3 cells/ml, were plated in 96-well plates and the plates were incubated for 24 hours. Following that, cells were exposed to a 100 μL aliquot of media containing SBG 5 at concentrations of 10

and 100 μg/ml. Following a 72-hour drug exposure period, the cells were fixed by substituting the media with 150 μL of 10% trichloroacetic acid (TCA) and incubated for one hour at 4 °C. Following the TCA solution removal, the cells underwent five rounds of distilled water washing. 70 μL aliquots of SRB solution (0.4% w/v) were added and incubated for 10 minutes at room temperature in a dark place. After being washed with 1% acetic acid three times, the plates were left to air dry overnight. Then, to dissolve the protein-bound SRB stain, 150 μL of tris aminomethane base solution (TRIS) (10 mM) was added, and the absorbance was measured at 540 nm using a FLUOstar® Omega Multi Detection Microplate Reader (BMG Labtech. Ortenberg, Germany) [69,70]. The test was repeated with an oral epithelial cell (OEC) cell line.

2.7 Clinical Study

The selection of patients was done in the Dermatology Department, Faculty of Medicine, Mansoura University Hospitals. 30 patients clinically diagnosed with *Tinea corporis* (TC) were selected for the study.

2.7.1 Patients

The inclusion criteria were patients of both genders with at least one TC skin lesion and displaying positive fungal skin scrapping with potassium hydroxide (KOH). The exclusion criteria were Pregnant and lactating women. Also, patients having HIV, any other life-threatening infection, or any medical condition that might have unacceptable risks were excluded.

2.7.2 Study design

This is a prospective, randomized, and controlled study. The eligible thirty patients who fulfilled the inclusion criteria were randomized into three treatment groups (1:1:1 ratio). Group I included patients treated topically with SBG 5 (1% Carbopol 940 hydrogel containing: SB 5 of 4.5% SP 60, 4.1 % CH, 1.6% SDC, and 2% STZ). Group II included patients treated topically with Dermofix® cream (2% STZ). Group III included patients treated topically with SAG (1% Carbopol 940 hydrogel containing 2% STZ). Patients were directed to apply the topical formulation to the lesions twice daily until complete recovery, or for a maximum period of 4 weeks. The efficiency and safety of SBG 5 in comparison to Dermofix® cream 2% and SAG 2% in the topical treatment

of TC were reported in the current study. Following the initial visit, the patients followed up every week during the treatment course. Clinical and mycological examinations were used for assessment of the treatment outcome.

2.7.3 Assessment of efficacy and safety

The efficacy and safety of SBG 5 were compared with Dermofix® cream 2% and SAG 2% for the positive clinical response and changes from baseline for the clinical parameters for evaluation of TC (signs and symptoms) that were reported every week by the clinical, visual and mycological examinations. The clinical parameters for evaluation of TC including pruritus, erythema, vesicles, and desquamation were assessed using a subjective score to assess the improvement degree according to the dermatologist's point of view. Five degrees of improvement were utilized; none (0% improvement), (minimal (25% improvement), mild (50% improvement), moderate (75% improvement), and complete improvement (100% improvement). The findings of the clinical examination were validated with the mycological microscopic examination of skin lesions based on the KOH test. A mycological cure from TC was considered with a negative KOH test [71,72]. Throughout the study, patients were asked to describe any discomfort or irritability, which allowed for the assessment of the safety of each treatment. The data are expressed as the mean ± standard deviation. The results were statistically evaluated using a non-parametric analysis of variance (Kruskal-Wallis test). $p < 0.05$ was considered statistically significant.

3. RESULTS AND DISCUSSION

3.1 Physicochemical *characteristics* of SBs

SBs were well prepared by the thin-film hydration technique combined with bath sonication. SBs showed PS (nm) ranging from 158.0 ± 6.4 to 561± 11.6 with a PDI of 0.16 ± 0.01 to 0.61 ± 0.01, ZP (mV) of −47.9 ± 0.6 to − 64.0 ± 1.6 and % EE of 68.7 ± 3.7 to 96.0 ± 3.4 (Table 2). PS, PDI, ZP, and % EE were previously reported to rely on the ratio of SP 60 to CH, as well as the type and concentration of bile salts [32,43,73,74]. Therefore, in this investigation, the effects of bile salts (SDC and DE) and CH on these parameters were examined by changing the SDC or DE amount, and the SP 60 to CH molar ratio, while maintaining an overall lipid content of 250 μmol.

Table 1. Composition of Sertaconazole bilosomes (SBs)

Formulation	Component				
	Molar ratio (SP 60:CH)	Type of Bile salt	SP 60 (mg)	CH (mg)	Bile Salt (mg)
SB 1	2:1	SDC	66.0	30.0	8.3
SB 2	1:1	SDC	49.5	44.5	8.3
SB 3	1:2	SDC	33.0	59.0	8.3
SB 4	2:1	SDC	60.0	27.0	16.6
SB 5	1:1	SDC	44.5	40.6	16.6
SB 6	1:2	SDC	30.0	54.0	16.6
SB 7	2:1	DE	66.0	30.0	8.5
SB 8	1:1	DE	49.5	44.5	8.5
SB 9	1:2	DE	33.0	59.0	8.5
SB 10	2:1	DE	60.0	27.0	17.0
SB 11	1:1	DE	44.5	40.6	17.0
SB 12	1:2	DE	30.0	54.0	17.0

SP 60, CH, SB, SDC, and DE indicate span 60, cholesterol, Sertaconazole-loaded bilosomes, sodium deoxycholate, and sodium dehydrocholate respectively. A total of 250 µmol of all lipid components (including SDC or DE, SP 60 and CH) was used in all formulations. A 20 mg of Sertaconazole nitrate was used in all formulations.

Table 2. Physicochemical characteristics of SBs (mean ± SD; n = 3)

Formulation	Evaluation parameter					
	PS (nm)	PDI	ZP (mv)	% EE	% Q_{8h}	% Q_{24h}
SB 1	224.4 ± 10.2	0.23 ± 0.02	-47.9 ± 0.6	83.1 ± 4.5	58.5 ± 2.9	76.4 ± 3.8
SB 2	180.8 ± 3.40	0.29 ± 0.02	-45.2 ± 4.2	88.5 ± 5.0	65.7 ± 2.6	88.5 ± 2.8
SB 3	196.3 ± 3.40	0.31 ± 0.02	-54.4 ± 2.0	78.1 ± 4.8	60.7 ± 2.4	84.9 ± 2.7
SB 4	303.4 ± 13.1	0.18 ± 0.03	-54.1 ± 0.9	90.2 ± 2.3	70.9 ± 2.8	96.0 ± 3.8
SB 5	158.0 ± 6.40	0.16 ± 0.01	-55.0 ± 1.7	96.0 ± 3.4	70.3 ± 3.6	97.2 ± 3.0
SB 6	164.2 ± 7.90	0.24 ± 0.02	-42.3 ± 2.2	80.3 ± 3.0	73.9 ± 4.4	100 ± 2.0
SB 7	493.5 ± 17.4	0.33 ± 0.11	-53.5 ± 3.4	76.6 ± 5.1	59.9 ± 3.0	85.8 ± 2.6
SB 8	315.8 ± 6.30	0.35 ± 0.03	-52.6 ± 0.4	90.3 ± 4.1	59.1 ± 3.3	79.8 ± 2.6
SB 9	561.1 ± 11.6	0.61 ± 0.01	-51.7 ± 2.2	87.9 ± 3.4	63.5 ± 2.9	83.5 ± 3.1
SB 10	384.9 ± 9.00	0.29 ± 0.04	-62.1 ± 4.1	79.6 ± 3.7	70.8 ± 3.5	98.0 ± 3.9
SB 11	460.0 ± 4.40	0.40 ± 0.01	-64.0 ± 1.6	85.2 ± 5.0	69.3 ± 4.3	99.2 ± 2.0
SB 12	465.9 ± 9.30	0.58 ± 0.07	-59.1 ± 2.3	68.7 ± 3.7	71.1 ± 4.3	99.3 ± 4.0

SB, PS, ZP, PDI, % EE, % Q_{8h}, and % Q_{24h} represent sertaconazole-loaded bilosomes, particle size, zeta potential, polydispersity index, % entrapment efficiency, % cumulative drug released after 8 hours, and % cumulative drug released after 24 hours respectively

3.1.1 Cholesterol effect

The CH composition seems to affect the PS and % EE of SBs. It was observed that in the formulations (SB 1 to SB 2, SB 4 to SB 5, or SB 7 to SB 8), the PS decreased in contrast to the increase in the CH proportion (Table 2). In general, CH regulates the stiffness and packing of the vesicles by interacting with the hydrophobic tails of the lipids in the vesicle bilayer [75]. So, the tight packing of the bilayers in the vesicles caused by the enhanced interactions between CH and SP 60 might be the cause of the PS decrease. In the formulations (SB 1 to SB 2, SB 4 to SB 5, SB 7 to SB 8, or SB 10 to SB 11), the % EE increased correspondingly with the CH proportion, indicating successful intercalation of STZ inside the bilayer with higher hydrophobic interactions and decreased STZ leakage from the rigid vesicles [75,76]. It's interesting to note that larger PS and lower % EE were observed following the further increase in the CH proportion in the formulations (SB 3, SB 6, SB 9, and SB 12). This could be explained by the disruption of the bilayer structure caused by the accommodation of the extra cholesterol, which could cause STZ to be expelled out of the vesicles [76, 77].

3.1.2 Bile salts effect

Bilosomes prepared with DE (SB 7-SB 12) had significantly larger PS than those prepared with SDC (SB 1-SB 6) (Table 2). This may be explained by the fact that vesicles having DE had noticeably higher ZP values. The vesicles with higher ZP would have a stronger repulsion force between the charged neighboring vesicular bilayers, increasing the distance between them, and causing comparatively larger vesicles to develop [78,79]. The % EE was lower in bilosomes with DE (SB 7-SB 12) compared to those with SDC (SB 1-SB 6). This could be related to the fact that SDC has higher hydrophobicity (HLB value = 16.0) than DE (HLB value = 25.0). Compared to vesicles containing DE, this enhanced hydrophobicity of SDC vesicles would allow the hydrophobic STZ to effectively intercalate inside the hydrophobic core of the bilayer, resulting in a larger % EE [80,81]. The PS of formulations with 40 μm (16.56 mg) SDC or (17 mg) DE (SB 5, SB 6, SB 10) were lower compared to those with 20 μm (8.3 mg) SDC or (8.5 mg) DE (SB 2, SB 3, SB 7), at similar molar ratios between SP 60 and CH. This revealed that the PS was dramatically reduced when the quantity of bile salts, in these molar ratios, was increased, which may be explained by the fact that bile salts, as anionic surfactants, reduce interfacial tension and cause smaller vesicles to form as a consequence [82]. The production of mixed micelles, which have smaller PS than vesicles as bile salt content increases, is another possible explanation [83-86]. The PS of SBs with 40 μm (16.56 mg) SDC or (17 mg) DE (SB 4, SB 11, SB 12) were lower compared to those with 20 μm (8.3 mg) SDC or (8.5 mg) DE (SB 1, SB 8, SB 9), at similar molar ratios between SP 60 and CH. These findings are consistent with earlier reports that showed that a larger PS would appear as a result of the repulsion between vesicle bilayers because of the presence of a greater ZP negative charge with the increased bile salt concentrations [78]. Furthermore, the extra SDC or DE that the bilayers accommodate might make the bilosomes bulkier, which increases the PS [87,88]. Remarkably, as the amount of bile salt increased, so did the % EE of STZ, which was consistent with the previous reports [74,89]. This might be because mixed micelle production increases the solubility of STZ in the medium of the prepared system [90]. The lipid bilayers of the vesicles were observed to fluidize at very high bile salt concentrations, which would lead the encapsulated drug to leak out [73,88,91].

3.2 *In vitro* Drug Release

The release profile of all the twelve SBs (58.5 and up to 73.9% % within 8 h and 76.4 and up to 100.0% % within 24 h) exhibited a biphasic process, displaying a quick burst at first, followed by a slower release phase, as shown in Fig. 1(a). This could be the result of STZ adsorbed on the vesicle's surface dissolving quickly in the dissolution medium, whereas the vesicle barrier effect was responsible for the slower phase [92-95]. Regardless of the molar ratio between SP 60 and CH or the kind of bile salt utilized, the amount of bile salt had a substantial effect on the drug release percentage (% Q_{8h} and % Q_{24h}) (Table 2). This could be due to the increase in bile salt amount, which would increase the fluidity of the lipid bilayer and permit more STZ to seep out [92,96-98]. The Korsmeyer-Peppas kinetic model was shown to have the best fit to the in vitro release data when compared to the zero-order, first-order, Hixson-Crowell, and Higuchi kinetic models, as indicated by the greatest coefficient of determination (R^2) (Table 3). Diffusion exponent "n" was found to be less than 0.45, suggesting that the Fickian diffusion process is applicable to SBs dispersions [92,99]. The SB 5 formulation showed uniformly distributed spherical bilosomes of 158 ± 6.4 nm, −55 ± 1.7mV, and 0.16 ± 0.01, for PS, ZP, and PDI, respectively, with higher % EE and % Q_{24h} (96 ± 3.4 and 97.2 ± 3.0 respectively). As a result, SB 5 formulation was optimized and used in further studies as well as for the preparation of SB 5-loaded hydrogel (SBG 5).

3.3 TEM

The transmission electron microscopy image, depicted in Fig. 2, showed layered spherical nanovesicles with a size range of 123–177 nm, which validated the vesicular structure of the optimized SB 5 formulation. Photon correlation spectroscopy only estimates the size of the nanovesicles based on scattered light and intensity, not their actual size [100,101]. Consequently, investigation using a transmission electron microscope is helpful in both verifying the findings from photon correlation spectroscopy and examining the morphology of SBs.

3.4 DSC

DSC thermograms of STZ, SP 60, CH, SDC, physical mixture, and the optimized formulation (SB 5) are presented in Fig. 3(A). DSC thermograms of STZ, SP 60, CH, and SDC

showed endothermic events at 159.2, 54.44, 149.8 and 116.27 °C respectively, corresponding to their melting temperatures [85,102-104]. The endothermic peak of STZ continued to exist in the physical mixture with some dilution effect but was missing in the optimized formulation (SB 5) thermogram. This observation might suggest that the physical state of STZ was transformed from crystalline to amorphous upon being integrated into the vesicular system [45,76]. The physical mixture thermogram showed that the fused peaks of SP 60, SDC, CH, and STZ were represented by a wide peak that ranged from 50 to 165 °C, while the optimized formulation (SB 5) thermogram showed a wide peak ranging from 50 to 150 °C, that represented the fused peaks of SP 60, SDC, and CH.
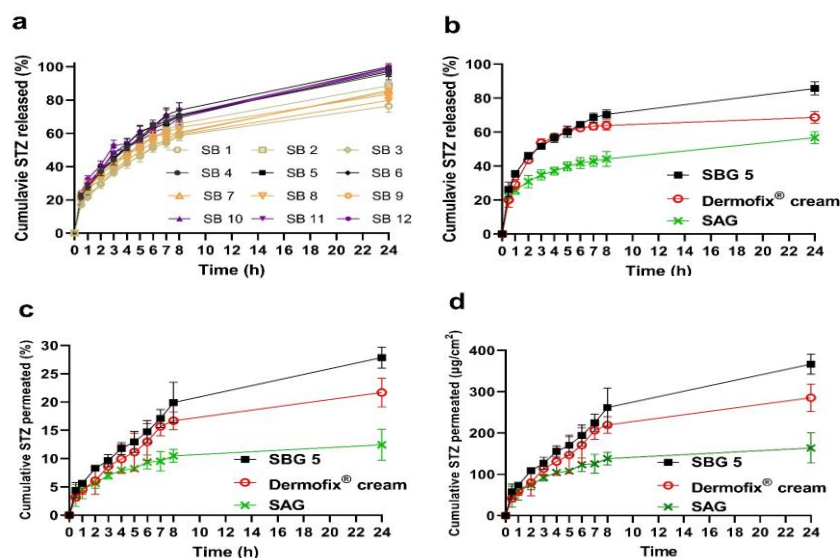

Fig. 1. In vitro release study of sertaconazole (STZ)-loaded bilosomes (SBs) (a). The in vitro release study (b) and the ex vivo permeation study (c and d) of the optimum sertaconazole-loaded bilosome hydrogel (SBG 5), marketed formulation (Dermofix® cream) and sertaconazole-alone hydrogel (SAG)
Each point represents the mean ± SD (n = 3)

Table 3. *In vitro* release kinetics of different SBs formulations, SBG 5, Dermofix® cream, and SAG

Formulation	Zero-order	First-order	Hixson-Crowell	Higuchi square root	Korsmeyer-Peppas	
	R^2				R^2	n
SB 1	0.697	0.884	0.826	0.947	0.992	0.364
SB 2	0.717	0.960	0.897	0.956	0.995	0.363
SB 3	0.765	0.963	0.912	0.974	0.995	0.408
SB 4	0.715	0.993	0.940	0.954	0.993	0.369
SB 5	0.730	0.997	0.959	0.962	0.994	0.380
SB 6	0.711	0.950	0.991	0.953	0.991	0.380
SB 7	0.714	0.947	0.885	0.952	0.996	0.346
SB 8	0.704	0.910	0.850	0.949	0.990	0.347
SB 9	0.672	0.910	0.840	0.933	0.996	0.322
SB 10	0.723	0.994	0.965	0.959	0.996	0.363
SB 11	0.759	0.981	0.984	0.974	0.998	0.385
SB 12	0.704	0.981	0.973	0.949	0.997	0.343
SAG	0.574	0.706	0.662	0.863	0.999	0.241
Dermofix® cream	0.405	0.518	0.478	0.739	0.945	0.255
SBG 5	0.572	0.866	0.771	0.875	0.989	0.285

R^2 and n represent coefficient of determination and diffusion exponent respectively
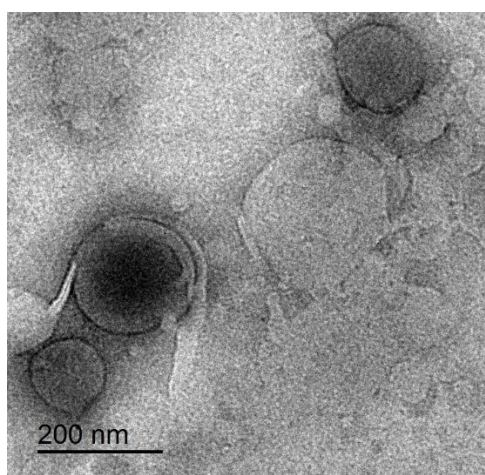
Fig. 2. Electron microscope image of sertaconazole-loaded bilosomes (SB 5)

3.5 FT-IR

FT-IR spectra of STZ, SP 60, CH, SDC, physical mixture, and the optimized formulation (SB 5) are portrayed in Fig. 3(B). STZ infrared spectra revealed bands at 1311 cm^{-1} (C-O ether stretch), 1462 cm^{-1} (C=C aromatic stretch), 1647 cm^{-1} (C=N aromatic stretch), and 3144 cm^{-1} (C-H stretch), as reported earlier [45]. An asymmetric and symmetric aliphatic C-H stretching at 2916 and 2849 cm^{-1} respectively, and a C=O stretching of the ester group at 1735 cm^{-1} were all seen with SP 60, along with an aliphatic OH stretching band at about 3392 cm^{-1}, as reported earlier [105]. Around 3400 cm^{-1} (OH stretching) and 2900 cm^{-1} (C–H stretching), bands of CH were observed, while SDC displayed bands at 2923, 2861 (C–H stretching), and 1562 (COO− stretching) cm^{-1}, as previously reported [45]. Fig. 3(B) illustrates how the STZ spectrum displays three distinct peaks at about 1311, 3144, and 1462 cm^{-1}. The distinctive peaks of STZ and other excipients did not significantly alter when the STZ spectrum was compared to the physical mixture and SB 5 spectra. Thus, it may be concluded that there is no interaction between STZ and the components of the vesicle membrane in SB 5 formulation [32,45].
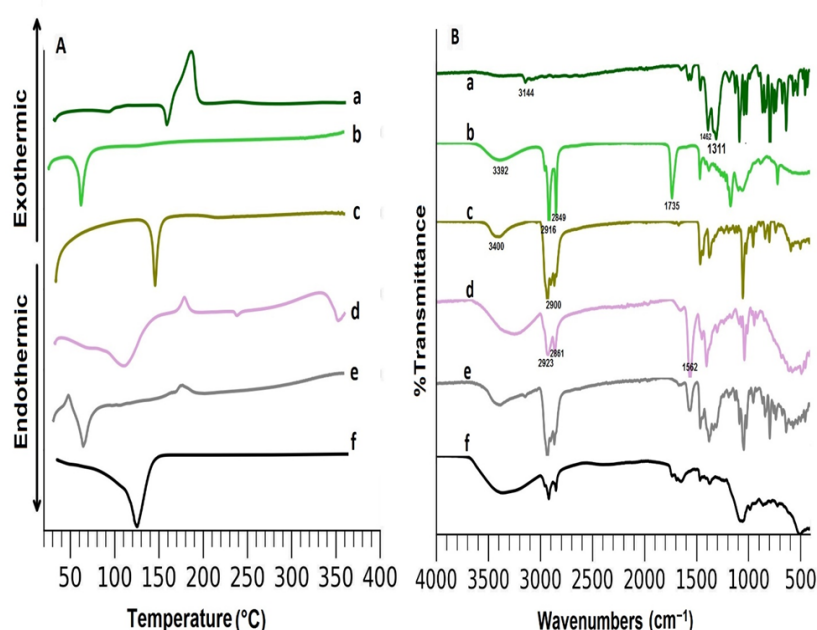

Fig. 3. DSC thermogram (A) and FT-IR spectra of (B) of STZ (a), SP 60 (b), CH (c), SDC (d), physical mixture (e), and SB 5 (f)

3.6 Stability Study

Table 4 specifies the stability parameters of the optimized SB 5 formulation at ambient and refrigerated (4 ± 1 °C) temperatures. After a month at ambient temperature, the PS, PDI, ZP, and % EE of SB 5 formulations were not altered statistically from the original observations, but they were significantly altered after six months ($p < 0.05$). This could be the result of bilosome aggregation along with STZ leaking [32]. SB 5 could be stored in a refrigerator at 4 ± 1 °C since there were no changes in PS, PDI, ZP, or % EE after six months of storage [106].

3.7 Evaluation of SBG 5

At a concentration of 1% w/w of Carbopol 940, SBG 5 displayed optimal viscosity. The drug content was determined to be within permissible limits, ranging from 97.87% to 99.34%. The pH was close to the skin's normal pH, ranging from 6.5 to 6.8. Therefore, for additional investigations on SBG 5, 1% hydrogel of Carbopol 940 was employed [67,107].

3.7.1 *In vitro* release study of SBG 5

The release profile of SBG 5, Dermofix® cream, and SAG ranged from 44.2 to 70.5% within 8 h and from 56.8 to 85.7% % within 24 h, as shown in Fig. 1(b). SBG 5 had a higher release percentage (70.5 and 85.7%) compared to Dermofix® cream (64.0 and 68.7) and SAG (44.2 and 56.8%) after 8 and 24 hours respectively. This significant increase in release percentage at 8 hours compared to SAG (1.60-fold) and at 24 hours compared to Dermofix® cream (1.25-fold) and SAG (1.51-fold) could be due to the presence of SDC in high amounts. In addition to its permeability-enhancing capability, SDC improves the fluidity and flexibility of the vesicle bilayer when introduced into the bilayer membrane, making it easier for STZ to escape from the vesicles [92,97]. The in vitro release data of SBG 5 were best fitted to the Korsmeyer–Peppas kinetic model according to the highest coefficient of determination (R^2) (0.989) (Table 3). The diffusion exponent "n" was found to be less than 0.45, suggesting that the Fickian diffusion process applies to SBG 5 [92,99].

3.7.2 Permeability and drug deposition study

3.7.2.1 Permeability study

The ex vivo STZ diffusion profiles of SBG 5, Dermofix® cream and SAG ranged from 10.3 to 19.4% within 8 h and from 12.5 to 27.7% % within 24 h, as shown in Fig. 1(c and d). SBG 5 had a higher cumulative STZ permeated (19.44 and 27.68 %) compared to Dermofix® cream (16.59 and 19.91) and SAG (10.32 and 12.50%) after 8 and 24 hours respectively. The cumulative STZ permeated from SBG 5 after 24 hours was found to be 366.7 ± 24.3 ug/cm², which was significantly higher ($p < 0.05$) than Dermofix® cream (285.4 ± 33.1 ug/cm²) and SAG (163.8 ± 36.3 µg/cm²) (Table 5). The SBG 5 flux was determined to be 15.3 µg/cm² /h, which was 1.4-fold higher than Dermofix® cream (10.9 µg/cm² /h) and 2.3-fold higher than SAG (6.8 µg/cm² /h) (Table 5). The nano-size of the vesicle and its significant internalization into the lipid matrix could be responsible for the permeation enhancement outcomes of SBG 5. Moreover, nonionic surfactants (SP 60) change the subcutaneous layer to facilitate vesicle penetration by enhancing the permeation capability as well as increasing the hydrostatic pressure [97,98]. Bile salt (SDC) breaks through intercellular lipids of the skin and overcomes the blockade property of the skin via its interaction with the coenocyte's keratin threads forcing it to open. In addition to improving vesicular elasticity and deformability, it may also lower the drug efflux from the skin [97,98,108-111].

3.7.2.2 Drug deposition study

Table 5 shows the result of STZ deposition from SBG 5, Dermofix® cream, and SAG. SBG 5 showed considerably more STZ deposition ($p < 0.05$) in the skin after a 24-hour treatment (16.3%) than Dermofix® cream (4.25%) and SAG (1.1%). SBG 5 showed a significantly higher drug deposition enhancement ratio (3.84-fold and 14.82-fold) concerning Dermofix® cream and SAG respectively, which could be due to the enhanced permeability through the stratum corneum and the ability to preserve the STZ reservoir effect in the skin layers in case of SBG 5 in contrary to the conventional systems due to the effect of SDC [65]. In topical skin treatment, the presence of higher drug levels in the skin would improve the efficacy. More drug retention in the skin allows for more effective treatment of deep tissue fungal infections [67]. Therefore, it may be suggested that SBG 5 could be more efficient in treating topical fungal infections than conventional systems.

Table 4. Physical stability of the optimized SB 5 formulation stored at ambient and refrigerated (4 ± 1 °C) temperatures (mean ± SD; n = 3)

Parameter		Storage time			
		zero time	1 month	3 months	6 months
Ambient temperature	PS (nm)	158.0 ± 6.4	174.9 ± 7.91	192.0 ± 5.41*	234.5 ± 5.22**
	PDI	0.16 ± 0.01	0.22 ± 0.02	0.272 ± 0.03*	0.283 ± 0.06*
	ZP (mV)	-55.05 ± 1.7	-53.83 ± 3.5	-49.37 ± 2.6	-46.56 ± 3.2*
	% EE	96.0 ± 3.4	91.3 ± 3.9	88.2 ± 2.5	84.5 ± 48*
Refrigerated temperature (4 ± 1 °C)	PS (nm)	158.0 ± 6.4	162.4 ± 4.71	167.1 ± 6.82	170.4 ± 7.30
	PDI	0.16 ± 0.01	0.19 ± 0.06	0.20 ± 0.05	0.23 ± 0.05
	ZP (mV)	-55.05 ± 1.7	-53.56 ± 2.4	-50.37 ± 4.0	-48.56 ± 4.5
	% EE	96.0 ± 3.4	94.8 ± 3.9	93.7 ± 2.8	91.6 ± 3.5

*$p < 0.05$, **$p < 0.005$ against the matching value at zero time*

Table 5. Permeability and drug deposition parameters of SBG 5, Dermofix® cream and SAG

Formulation	Permeability				Deposition	
	D_{24h} (µg.cm^{-2})	Flux (µg.cm^{-2}.h^{-1})	$P_{app} \times 10^{-4}$ (cm.h^{-1})	ER	DD%	ER$_{DD}$
SAG	163.8 ± 36.3	6.8	3.4	_	1.10 ± 0.6	_
Dermofix® cream	285.4 ± 33.1	10.9	5.5	1.6	4.25 ± 2.31	3.86
SBG 5	366.7 ± 24.3	15.3	7.7	2.3	16.30 ± 3.12	14.82

SAG, SBG 5, D_{24h}, P_{app}, ER, DD%, and ER$_{DD}$ represent Sertaconazole-alone hydrogel, the optimum Sertaconazole-loaded bilosome hydrogel, cumulative Sertaconazole permeated after 24 hours per unit area (µg/cm^2), apparent permeability co-efficient, permeability enhancement ratio, % drug deposition, and drug deposition enhancement ratio respectively

3.8 Microbiological Efficacy Assessment Study

The in vitro antifungal properties of SBG 5, Dermofix® cream, and SAG were assessed through the agar well diffusion technique against Ca, Ab and Sc as an indicator for the antifungal activity [112]. Zones of inhibition are the clear rings that start to form around the dishes. The more effective the formulation, the bigger the zone of inhibition. It is noted that the plain formula used in this study showed no antifungal activity. The results represented in Fig. 4(a) revealed that zones of inhibition against Ca were 10.5 ± 0.3, 5.4 ± 0.2, and 7.3 ± 0.2 mm for SBG 5, Dermofix® cream, and SAG respectively. From the results, it is clear that the developed SBG 5 was more effective than the tested commercial formulation (Dermofix® cream) (two-fold) and drug alone hydrogel (SAG) (1.4-fold) suggesting higher efficacy against Cutaneous candidiasis caused by *Ca* [113]. Zones of inhibition against Ab, as shown in Fig. 4(b), and Sc, as shown in Fig. 4(c), were 7.7 ± 0.1 and 20.8 ± 0.2 mm, 7.3 ± 0.2 and 17.0 ± 0.2 mm, and 5.4 ± 0.2 and 14.5

± 0.2 mm for SBG 5, Dermofix® cream and SAG respectively, as shown in f. SBG 5 exhibited anti-fungal efficacy against Ab (1.4-fold) higher than SAG suggesting higher efficacy against ocular keratitis and non-dermatophyte mold onychomycosis (NDMO) caused by Ab [114,115]. Also, SBG 5 exhibited anti-fungal efficacy against Sc (1.4-fold) higher than SAG suggesting higher efficacy against numerous cases of *S. cerevisiae*-induced vaginitis and oropharyngeal infection [116]. From the results of in vitro antifungal activity, it is clear that the developed SBG 5 was more effective than the drug alone formulation (SAG) in the same degree (1.4-fold) against the three fungi used (Ca, Ab and Sc), which may be attributed to the penetration enhancer effect of the bile salt (SDC) and the encapsulation properties of the vesicles leading to the higher in vitro release, permeability and drug deposition potential of SBG 5, in comparison with SAG as discussed earlier. As a result, the concentration gradient across the fungal cell wall increased, allowing more STZ to come into contact with the fungal cell, and effectively inhibit the ergosterol synthesis [27].

This suggests the promising approach of bilosomes to magnify the antifungal potential of STZ topically.

3.9 Cytotoxicity Assay

The in vitro cytotoxicity study was performed to evaluate the safety of SBG 5 formulation. The SRB colorimetric assay is the recommended approach among currently available methods for in vitro cytotoxicity screening studies as it offers increased reproducibility and linearity, less susceptibility to changes in the environment, and independence from intermediary metabolism. [117]. The SRB assay offers reduced variance between cell lines in addition to increased

sensitivity [118]. HSF and OEC cell lines were utilized in the cytotoxicity assay, which provides a useful model for the topical application of the SBG 5 formulation on the skin. As seen in Fig. 5, SBG 5 did not exhibit any noticeable toxicity against HSF and OEC cells at the used concentrations, preserving cell viability > 99.4% and 97.43%, respectively, in comparison to untreated HSF and OEC. Positive controls (cisplatin and doxorubicin) were used to verify the validity of the experimental conditions. At the same utilized concentrations, cisplatin showed % cell viability of 42 and 67.84%, and doxorubicin showed % cell viability of 55.64 and 39.03% against HSF and OEC respectively.
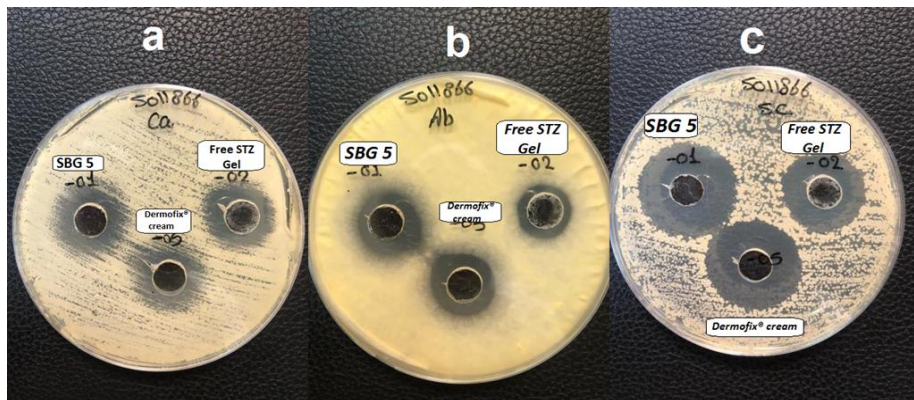

Fig. 4. Microbiological activity of SBG 5, Dermofix® cream and SAG against *Candida albicans* (a), *Aspergillus brasiliensis* (b) and *Saccharomyces cerevisiae* (c) using agar diffusion technique
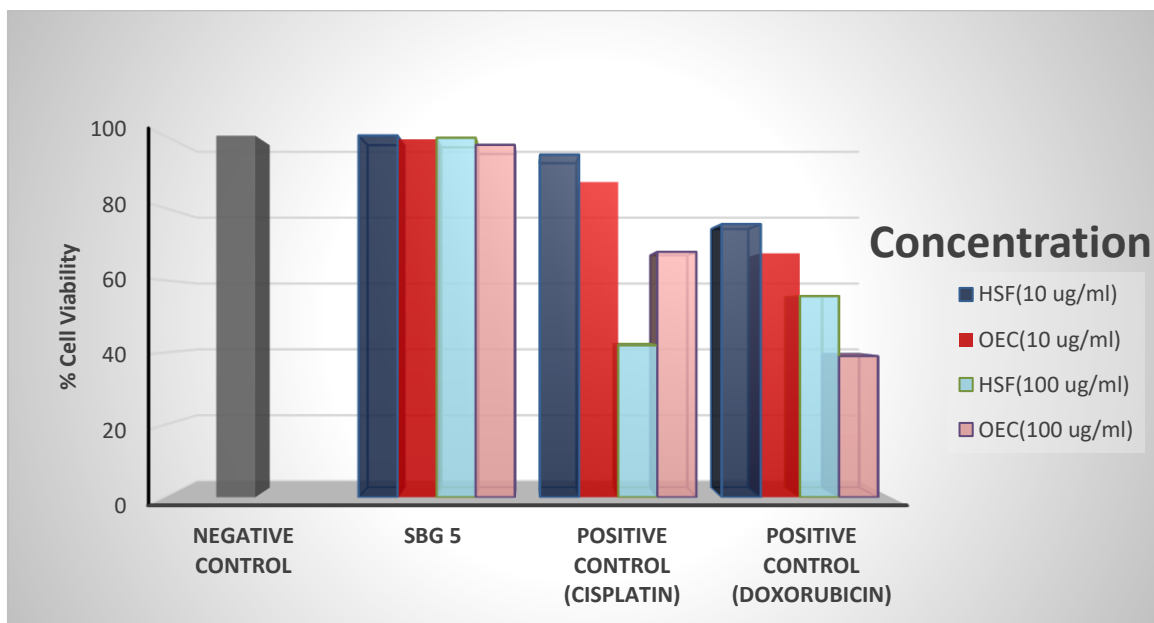

Fig. 5. Cytotoxicity profile of SBG 5 in HSF and OEC cell lines

3.10 Clinical Study

All 30 patients with TC presented with circinate erythematous scaly lesions with elevated raised borders on the trunk and extremities. The diagnosis was positively confirmed when positive KOH scraping showed fungal elements in the shape of hyphae. After 14 days of treatment, 90% of patients receiving SBG 5 experienced a full cure (100% improvement), compared to 50% of patients receiving Dermofix® cream and 20% of those receiving SAG (Fig. 6). After 21 days of treatment, 100% of patients having SBG 5 experienced a full recovery, compared to 80% of patients receiving Dermofix® cream and 50% of patients receiving SAG. After being evaluated by the dermatologist, SBG 5 exhibited a cure rate that was 1.8 times higher at day 14 and 1.25 times higher at day 21 than Dermofix® cream. Day 14 and 21 cure rates for SBG 5 were 4.5 and 2 times respectively, higher than those of SAG. Comparing SBG 5 to Dermofix® cream and SAG, the patients cure rate was statistically improved on days 14 and 21. Table 6 represents the different clinical parameters and overall response of different treatments used in the study. There is a significant difference between the three formulations in all clinical parameters included, overall response, and duration of complete improvement as shown in Table 6 with SBG 5 showing the better performance. Fig. 7

represents a TC lesion in a patient before and after treatment with SBG 5. Since it is commonly recognized that an antifungal agent's concentration in the target organ determines its therapeutic performance, SBG 5 was also able to markedly increase STZ deposition and accumulation in deeper layers of the skin. The deep skin penetrating potential of STZ from SBG 5 formulation is confirmed by the presence of a specific percentage of STZ (27.68 %) in the modified Franz diffusion receptor compartment compared to 19.91% STZ with Dermofix® cream and 12.50% with SAG as reported earlier in ex-vivo permeability study. The reason for this could be that STZ was able to enter the epidermis more freely and flexibly due to the bilosomes deformability [31]. Also, the earlier skin deposition study showed 16.30% STZ skin deposition from SBG 5 compared to 4.25% with Dermofix® cream and 1.10% with SAG. The ex-vivo skin deposition study has demonstrated that a significant amount of the drug accumulates in skin layers, which may account for the fast onset of action. Clinical trials performed on TC patients demonstrated the advantages of nanovesicles over free drug-containing gel and traditional topical therapy creams in curing such fungal infections. The ability of the bilosome vesicles to enhance the antifungal potential of STZ is suggested by the fact that SBG 5 outperformed Dermofix® cream and SAG in terms of cure
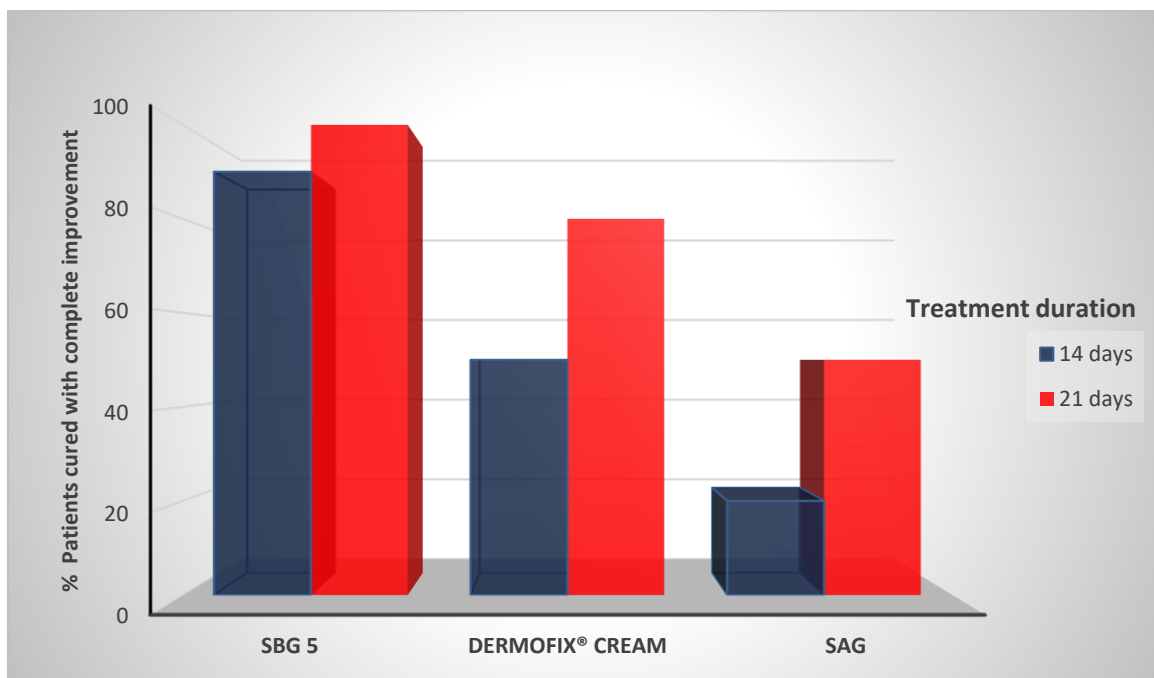

Fig. 6. % Patients cured with complete improvement treated with SBG 5, Dermofix® cream and SAG for 14 and 21 days

Table 6. Summary of the different clinical parameters with respect to different treatment formulations (% improvement)

Formulation	Erythema	Pruritus	Vesicles	Desquamation	Overall response	Duration of treatment in weeks
SAG	80.00 ± 7.50	78.00 ± 2.7	75.00 ± 5.3	82.50 ± 4.5	81.5 ± 6.3	3.0 ± 0.7
Dermofix® cream	83.13 ± 10.5	88.75 ± 8.5	91.00 ± 1.0	90.00 ± 2.4	91.0 ± 3.2	2.7 ± 0.8
SBG 5	95.00 ± 4.20	97.50 ± 5.0	98.75± 2.5	93.75 ± 12.5	95.0 ± 5.0	1.7 ± 0.5
*p value	.001	.001	.001	.002	.001	.003

Mean of ten patients ± SD, Significance difference at p < 0.05

Fig. 7. Photographic pictures before and after treatment with SBG 5

magnitude and rate. The TC lesions healed more quickly with SBG 5, which had an equivalent dosage of STZ to the commercial Dermofix® cream and SAG. Pharmacologically, the presence of bile salt (SDC) and the fact that the SDC is present in small vesicles (158.0 ± 6.40 nm) may contribute to the vesicles' improved skin penetrability. However, the small number of patients on which the investigation was conducted is a drawback of this clinical study. As a result, we advise conducting more extensive research in the future [119].

4. CONCLUSION

SBs were successfully produced and evaluated. Small, spherical, uniformly dispersed vesicles with greater percentages of % EE, ZP, % Q_{8h}, and % Q_{24h} were formed by the SB 5 with an equimolar ratio between the vesicular components and a higher proportion of bile salt (SDC). The optimized SB 5 formulation was refrigerated for six months at 4 ± 1 °C and showed good stability throughout this period. The optimized SB 5-loaded hydrogel (SBG 5) performed better in terms of the in vitro drug release, permeability, skin deposition characteristics, and antifungal activity than the commercial formulation (Dermofix® cream) and

STZ alone hydrogel (SAG). The in vitro cytotoxicity study was performed on human skin fibroblast (HSF) and oral epithelial cell (OEC) cell lines, and the safety of SBG 5 formulation for topical application on humans was confirmed. The clinical study showed that SBG 5, outperformed Dermofix® cream and SAG in terms of the magnitude and rate of healing of *Tinea corporis* lesions. Therefore, SBG 5 is considered a good option for a more extensive clinical study down the road.

DISCLAIMER (ARTIFICIAL INTELLIGENCE)

Author(s) hereby declare that NO generative AI technologies such as Large Language Models (ChatGPT, COPILOT, etc) and text-to-image generators have been used during writing or editing of manuscripts.

CONSENT

All authors declare that written informed consent was obtained from the patient.

ETHICAL APPROVAL

All authors hereby declare that all experiments have been examined and approved by The

Ethical Committee of the Faculty of Pharmacy, Mansoura University, Mansoura, Egypt (Ethical Approval Code 2024-27).

COMPETING INTERESTS

Authors have declared that no competing interests exist.

REFERENCES

1. Piérard GE, Arrese JE, Piérard-Franchimont C. Treatment and prophylaxis of tinea infections. Drugs. 1996;52:209-24.
2. Kumar N, Goindi S. Statistically designed nonionic surfactant vesicles for dermal delivery of itraconazole: characterization and in vivo evaluation using a standardized Tinea pedis infection model. Int J Pharm. 2014;472(1-2):224-40.
3. Detandt M, Nolard N. Fungal contamination of the floors of swimming pools, particularly subtropical swimming paradises. Mycoses. 1995;38(11-12):509-13.
4. Brown GD, Denning DW, Gow NAR, Levitz SM, Netea MG, White TC. Hidden Killers: Human Fungal Infections. Science Translational Medicine. 2012;4(165): 165rv 13-rv13.
5. Ekowati Y, Ferrero G, Kennedy MD, de Roda Husman AM, Schets FM. Potential transmission pathways of clinically relevant fungi in indoor swimming pool facilities. Int J Hyg Environ Health. 2018;221(8):1107-15.
6. Aggarwal N, Goindi S. Preparation and evaluation of antifungal efficacy of griseofulvin loaded deformable membrane vesicles in optimized guinea pig model of Microsporum canis--dermatophytosis. Int J Pharm. 2012;437(1-2):277-87.
7. Branscomb R. The Dermatophytoses. Laboratory Medicine. 2005;36(8):496-500.
8. Barros M, Santos DA, Hamdan JS. Evaluation of susceptibility of Trichophyton mentagrophytes and Trichophyton rubrum clinical isolates to antifungal drugs using a modified CLSI microdilution method (M38-A). J Med Microbiol. 2007;56(Pt 4):514-8.
9. Makimura K, Mochizuki T, Hasegawa A, Uchida K, Saito H, Yamaguchi H. Phylogenetic classification of Trichophyton mentagrophytes complex strains based on DNA sequences of nuclear ribosomal internal transcribed spacer 1 regions. Journal of Clinical Microbiology. 1998;36 (9):2629-33.
10. Santos D, Hamdan J. Evaluation of broth microdilution antifungal susceptibility testing conditions for Trichophyton rubrum. Journal of Clinical microbiology. 2005;43 (4):1917-20.
11. Torres J, Marquez M, Camps F. Sertaconazole in the treatment of mycoses: from dermatology to gynecology. Int J Gynaecol Obstet. 2000;71 Suppl 1:S3-20.
12. Pfaller MA, Sutton DA. Review of in vitro activity of sertaconazole nitrate in the treatment of superficial fungal infections. Diagn Microbiol Infect Dis. 2006;56(2):147-52.
13. Agut J, Palacín C, Sacristán A, Ortiz J. Inhibition of ergosterol synthesis by sertaconazole in Candida albicans. Arzneimittelforschung. 1992;42(5A):718-20.
14. Palacín C, Sacristán A, Ortiz JA. In vitro comparative study of the fungistatic and fungicidal activity of sertaconazole and other antifungals against Candida albicans. Arzneimittelforschung. 1992;42(5A):711-4.
15. Del Rosso JQ. Comprehensive management of patients with superficial fungal infections: the role of sertaconazole nitrate. Cutis. 2008;81(6 Suppl):4-18; quiz 9-20.
16. Carrillo-Muñoz AJ, Giusiano G, Ezkurra PA, Quindós G. Sertaconazole: updated review of a topical antifungal agent. Expert Review of Anti-infective Therapy. 2005;3 (3):333-42.
17. Sanchez J. Sertaconazole, mechanism of action and pharmacokinetics. J Eur Acad Dermatol Venereol. 1993;2(Suppl 2):S71-6.
18. Guarro J, Figueras MJ, Cano J. Alterations Produced by Sertaconazole on the Morphology and Ultrastructure of Candida albicans: Sertaconazol-bedingte Veranderungen der Morphologie und Ultrastruktur von Candida albicans. Mycoses. 1989;32(6):283-95.

19. Agut J, Palacín C, Salgado J, Casas E, Sacristán A, Ortiz JA. Direct membrane-damaging effect of sertaconazole on Candida albicans as a mechanism of its fungicidal activity. Arzneimittelforschung. 1992;42(5A):721-4.

20. Savin R, Jorizzo J. The safety and efficacy of sertaconazole nitrate cream 2% for tinea pedis. CUTIS-NEW YORK-. 2006;78(4): 268.

21. Nasarre J, Umbert P, Herrero E, Roset P, Márquez M, Torres J, et al. Therapeutic efficacy and safety of the new antimycotic sertaconazole in the treatment of pityriasis versicolor. Arzneimittelforschung. 1992;42 (5A):764-7.

22. Borelli C, Klövekorn G, Ernst T-M, Bödeker R-H, Korting HC, Neumeister C. Comparative study of 2% sertaconazole solution and cream formulations in patients with tinea corporis, tinea pedis interdigitalis, or a corresponding candidosis. American journal of clinical dermatology. 2007;8:371-8.

23. Lopez-Montero E, Santos J-FRd, Torres-Labandeira JJ, Concheiro A, Alvarez-Lorenzo C. Sertaconazole-Loaded Cyclodextrin–Polysaccharide Hydrogels as Antifungal Devices §. The Open Drug Delivery Journal. 2009;3(1).

24. Güng S. New formulation strategies in topical antifungal therapy; 2013.

25. Lee CM, Maibach HI. Deep percutaneous penetration into muscles and joints. Journal of pharmaceutical sciences. 2006; 95(7):1405-13.

26. Younes NF, Abdel-Halim SA, Elassasy AI. Solutol HS15 based binary mixed micelles with penetration enhancers for augmented corneal delivery of sertaconazole nitrate: optimization, in vitro, ex vivo and in vivo characterization. Drug Deliv. 2018; 25(1): 1706-17.

27. Radwan SAA, ElMeshad AN, Shoukri RA. Microemulsion loaded hydrogel as a promising vehicle for dermal delivery of the antifungal sertaconazole: design, optimization and ex vivo evaluation. Drug Dev Ind Pharm. 2017;43(8):1351-65.

28. Esenturk I, Gumrukcu S, Özdabak Sert AB, Kök FN, Döşler S, Gungor S, et al. Silk-fibroin-containing nanofibers for topical sertaconazole delivery: preparation, characterization, and antifungal activity.

29. Kumar L, Verma S, Bhardwaj A, Vaidya S, Vaidya B. Eradication of superficial fungal infections by conventional and novel approaches: a comprehensive review. Artificial Cells, Nanomedicine, and Biotechnology. 2014;42(1):32-46.

30. Imam SS, Gilani SJ, Zafar A, Jumah MNB, Alshehri S. Formulation of Miconazole-Loaded Chitosan-Carbopol Vesicular Gel: Optimization to In Vitro Characterization, Irritation, and Antifungal Assessment. Pharmaceutics. 2023;15(2).

31. Al-Mahallawi AM, Abdelbary AA, Aburahma MH. Investigating the potential of employing bilosomes as a novel vesicular carrier for transdermal delivery of tenoxicam. Int J Pharm. 2015;485(1-2):329-40.

32. Janga KY, Tatke A, Balguri SP, Lamichanne SP, Ibrahim MM, Maria DN, et al. Ion-sensitive in situ hydrogels of natamycin bilosomes for enhanced and prolonged ocular pharmacotherapy: in vitro permeability, cytotoxicity and in vivo evaluation. Artif Cells Nanomed Biotechnol. 2018;46(sup1):1039-50.

33. Shukla A, Mishra V, Kesharwani P. Bilosomes in the context of oral immunization: development, challenges and opportunities. Drug Discov Today. 2016;21(6):888-99.

34. Kaurav H, Tripathi M, Kaur SD, Bansal A, Kapoor DN, Sheth S. Emerging Trends in Bilosomes as Therapeutic Drug Delivery Systems. Pharmaceutics. 2024;16(6):697.

35. Ammar HO, Mohamed MI, Tadros MI, Fouly AA. High frequency ultrasound mediated transdermal delivery of ondansetron hydrochloride employing bilosomal gel systems: ex-vivo and in-vivo characterization studies. Journal of Pharmaceutical Investigation. 2020;50: 613-24.

36. Wang L, Huang X, Jing H, Ma C, Wang H. Bilosomes as effective delivery systems to improve the gastrointestinal stability and bioavailability of epigallocatechin gallate (EGCG). Food research international. 2021;149:110631.

37. Chai C, Park J. Food liposomes: Structures, components, preparations, and applications. Food Chemistry. 2024;432: 137228.

International Journal of Polymeric Materials and Polymeric Biomaterials. 2020;70(9):605-22.

38. Saifi Z, Rizwanullah M, Mir SR, Amin S. Bilosomes nanocarriers for improved oral bioavailability of acyclovir: A complete characterization through in vitro, ex-vivo and in vivo assessment. Journal of Drug Delivery Science and Technology. 2020;57.

39. Duangjit S, Opanasopit P, Rojanarata T, Ngawhirunpat T. Evaluation of meloxicam-loaded cationic transfersomes as transdermal drug delivery carriers. AAPS PharmSciTech. 2013;14(1):133-40.

40. Elkomy MH, Alruwaili NK, Elmowafy M, Shalaby K, Zafar A, Ahmad N, et al. Surface-modified bilosomes nanogel bearing a natural plant alkaloid for safe management of rheumatoid arthritis inflammation. Pharmaceutics. 2022;14(3): 563.

41. Chng C-P, Hsia KJ, Huang C. Modulation of lipid vesicle–membrane interactions by cholesterol. Soft Matter. 2022;18(40):7752-61.

42. Zarenezhad E, Marzi M, Abdulabbas HT, Jasim SA, Kouhpayeh SA, Barbaresi S, et al. Bilosomes as nanocarriers for the drug and vaccine delivery against gastrointestinal infections: Opportunities and challenges. Journal of Functional Biomaterials. 2023;14(9):453.

43. Aziz DE, Abdelbary AA, Elassasy AI. Investigating superiority of novel bilosomes over niosomes in the transdermal delivery of diacerein: in vitro characterization, ex vivo permeation and in vivo skin deposition study. J Liposome Res. 2019;29(1):73-85.

44. Manconi M, Sinico C, Caddeo C, Vila AO, Valenti D, Fadda AM. Penetration enhancer containing vesicles as carriers for dermal delivery of tretinoin. Int J Pharm. 2011;412(1-2):37-46.

45. Abdellatif MM, Khalil IA, Khalil MAF. Sertaconazole nitrate loaded nanovesicular systems for targeting skin fungal infection: In-vitro, ex-vivo and in-vivo evaluation. Int J Pharm. 2017;527(1-2):1-11.

46. Manjunath K, Venkateswarlu V, Hussain A. Preparation and characterization of nitrendipine solid lipid nanoparticles, Pharmazie, 66, 178-186 (2011).

47. Hintz RJ, Johnson KC. The effect of particle size distribution on dissolution rate and oral absorption. International Journal of Pharmaceutics. 1989;51(1):9-17.

48. Dressman JB, Fleisher D, Amidon GL. Physicochemical Model for Dose-Dependent DrugAbsorption. Journal of Pharmaceutical Sciences. 1984;73(9): 1274-9.

49. Noyes AA, Whitney WR. The rate of solution of solid substances in their own solutions. Journal of the American Chemical Society. 1897;19(12): 930-4.

50. Gencturk A, Kahraman E, Güngör S, Özhan G, Özsoy Y, Sarac AS. Polyurethane/hydroxypropyl cellulose electrospun nanofiber mats as potential transdermal drug delivery system: characterization studies and in vitro assays. Artificial Cells, Nanomedicine, and Biotechnology. 2017;45(3):655-64.

51. Dash S, Murthy PN, Nath L, Chowdhury P. Kinetic modeling on drug release from controlled drug delivery systems. Acta Pol Pharm. 2010;67(3):217-23.

52. Elmoghayer ME, Saleh NM, Abu H, II. Enhanced oral delivery of hesperidin-loaded sulfobutylether-beta-cyclodextrin/ chitosan nanoparticles for augmenting its hypoglycemic activity: in vitro-in vivo assessment study. Drug Deliv Transl Res. 2024;14(4):895-917.

53. Gabr YA, Girgis GNS, El-Sabbagh HM. Surface-Decorated Nanocarrier as a Targeted Drug Delivery Cargo to Folate Receptor-Overexpressing Cells for Enhancing Anti-cancer and Anti-inflammatory Activity. Journal of Pharmaceutical Research International. 2023;35(18):41-74.

54. Younes NF, Abdel-Halim SA, Elassasy AI. Corneal targeted Sertaconazole nitrate loaded cubosomes: Preparation, statistical optimization, in vitro characterization, ex vivo permeation and in vivo studies. Int J Pharm. 2018;553(1-2):386-97.

55. El-Nabarawi M, Khalil I, Saad R. Impact of hydrophilic polymer solubilization on bioavailability enhancement of repaglinide by solid dispersion. Inven Rapid Pharm Tech. 2016;3:1-12.

56. Bsieso EA, Nasr M, Moftah NH, Sammour OA, Gawad NAAE. Could nanovesicles containing a penetration enhancer clinically improve the therapeutic outcome in skin fungal diseases? Nanomedicine. 2015;10 (13):2017-31.

57. Duvnjak Romić M, Sušac A, Lovrić J, Cetina-Čižmek B, Filipović-Grčić J, Hafner A. Evaluation of stability and in vitro wound healing potential of melatonin loaded (lipid enriched) chitosan based microspheres. Acta Pharmaceutica. 2019;69(4):635-48.

58. Zhu W, Guo C, Yu A, Gao Y, Cao F, Zhai G. Microemulsion-based hydrogel formulation of penciclovir for topical delivery. Int J Pharm. 2009;378(1-2):152-8.

59. Lei W, Yu C, Lin H, Zhou X. Development of tacrolimus-loaded transfersomes for deeper skin penetration enhancement and therapeutic effect improvement in vivo. Asian Journal of Pharmaceutical Sciences. 2013;8(6):336-45.

60. Sahoo S, Pani NR, Sahoo SK. Effect of microemulsion in topical sertaconazole hydrogel: in vitro and in vivo study. Drug Deliv. 2016;23(1):338-45.

61. R As, Sirivat A, Vayumhasuwan P. Viscoelastic properties of Carbopol 940 gels and their relationships to piroxicam diffusion coefficients in gel bases. Pharm Res. 2005;22(12):2134-40.

62. Shirsand S, Para M, Nagendrakumar D, Kanani K, Keerthy D. Formulation and evaluation of Ketoconazole niosomal gel drug delivery system. Int J Pharm Investig. 2012;2(4):201-7.

63. Tavakoli N, Taymouri S, Saeidi A, Akbari V. Thermosensitive hydrogel containing sertaconazole loaded nanostructured lipid carriers for potential treatment of fungal keratitis. Pharm Dev Technol. 2019;24 (7):891-901.

64. Trombino S, Russo R, Mellace S, Varano GP, Laganà AS, Marcucci F, et al. Solid lipid nanoparticles made of trehalose monooleate for cyclosporin-A topic release. Journal of Drug Delivery Science and Technology. 2019;49:563-9.

65. Garg BJ, Garg NK, Beg S, Singh B, Katare OP. Nanosized ethosomes-based hydrogel formulations of methoxsalen for enhanced topical delivery against vitiligo: formulation optimization, in vitro evaluation and preclinical assessment. J Drug Target. 2016;24(3):233-46.

66. Majumdar S, Srirangam R. Solubility, Stability, Physicochemical Characteristics and In Vitro Ocular Tissue Permeability of Hesperidin: A Natural Bioflavonoid. Pharmaceutical Research. 2008;26(5): 1217-25.

67. Bikkad ML, Nathani AH, Mandlik SK, Shrotriya SN, Ranpise NS. Halobetasol propionate-loaded solid lipid nanoparticles (SLN) for skin targeting by topical delivery. J Liposome Res. 2014;24(2):113-23.

68. Barot BS, Parejiya PB, Patel HK, Gohel MC, Shelat PK. Microemulsion-based gel of terbinafine for the treatment of onychomycosis: optimization of formulation using D-optimal design. AAPS PharmSciTech. 2012;13(1):184-92.

69. Abdellatif MM, Elakkad YE, Elwakeel AA, Allam RM, Mousa MR. Formulation and characterization of propolis and tea tree oil nanoemulsion loaded with clindamycin hydrochloride for wound healing: In-vitro and in-vivo wound healing assessment. Saudi Pharm J. 2021;29(11):1238-49.

70. Skehan P, Storeng R, Scudiero D, Monks A, McMahon J, Vistica D, et al. New Colorimetric Cytotoxicity Assay for Anticancer-Drug Screening. JNCI: Journal of the National Cancer Institute. 1990;82 (13):1107-12.

71. Ruocco E, Baroni A, Donnarumma G, Ruocco V. Diagnostic procedures in dermatology. Clin Dermatol. 2011;29(5): 548-56.

72. Andrews MD, Burns M. Common tinea infections in children. Am Fam Physician. 2008;77(10):1415-20.

73. Abdelbary AA, Abd-Elsalam WH, Al-Mahallawi AM. Fabrication of novel ultradeformable bilosomes for enhanced ocular delivery of terconazole: In vitro characterization, ex vivo permeation and in vivo safety assessment. Int J Pharm. 2016;513(1-2):688-96.

74. Ammar HO, Mohamed MI, Tadros MI, Fouly AA. Transdermal Delivery of Ondansetron Hydrochloride via Bilosomal Systems: In Vitro, Ex Vivo, and In Vivo Characterization Studies. AAPS PharmSciTech. 2018;19(5):2276-87.

75. Zhang J, Xue R, Ong WY, Chen P. Roles of cholesterol in vesicle fusion and motion. Biophys J. 2009;97(5):1371-80.

76. Janga KY, Jukanti R, Velpula A, Sunkavalli S, Bandari S, Kandadi P, et al. Bioavailability enhancement of zaleplon via proliposomes: Role of surface charge. Eur J Pharm Biopharm. 2012;80(2):347-57.

77. Kakkar S, Kaur IP. Spanlastics--a novel nanovesicular carrier system for ocular delivery. Int J Pharm. 2011;413(1-2):202-10.

78. El Zaafarany GM, Awad GA, Holayel SM, Mortada ND. Role of edge activators and surface charge in developing ultradeformable vesicles with enhanced skin delivery. Int J Pharm. 2010;397(1-2): 164-72.

79. Abdelbary G. Ocular ciprofloxacin hydrochloride mucoadhesive chitosan-coated liposomes. Pharm Dev Technol. 2011;16(1):44-56.

80. Abdelbary GA, Aburahma MH. Oro-dental mucoadhesive proniosomal gel formulation loaded with lornoxicam for management of dental pain. J Liposome Res. 2015;25 (2):107-21.

81. Kunieda H, Ohyama K-i. Three-phase behavior and HLB numbers of bile salts and lecithin in a water-oil system. Journal of Colloid and Interface Science. 1990; 136(2):432-9.

82. Dora CP, Singh SK, Kumar S, Datusalia AK, Deep A. Development and characterization of nanoparticles of glibenclamide by solvent displacement method. Acta pol pharm. 2010;67(3):283-90.

83. Al-Mahallawi AM, Khowessah OM, Shoukri RA. Nano-transfersomal ciprofloxacin loaded vesicles for non-invasive trans-tympanic ototopical delivery: in-vitro optimization, ex-vivo permeation studies, and in-vivo assessment. Int J Pharm. 2014;472(1-2):304-14.

84. van den Bergh BAI, Wertz PW, Junginger HE, Bouwstra JA. Elasticity of vesicles assessed by electron spin resonance, electron microscopy and extrusion measurements. International Journal of Pharmaceutics. 2001;217(1):13-24.

85. Basha M, Abd El-Alim SH, Shamma RN, Awad GE. Design and optimization of surfactant-based nanovesicles for ocular delivery of Clotrimazole. J Liposome Res. 2013;23(3):203-10.

86. Salama HA, Mahmoud AA, Kamel AO, Abdel Hady M, Awad GA. Phospholipid based colloidal poloxamer-nanocubic vesicles for brain targeting via the nasal route. Colloids Surf B Biointerfaces. 2012; 100:146-54.

87. Salama HA, Mahmoud AA, Kamel AO, Abdel Hady M, Awad GA. Brain delivery of olanzapine by intranasal administration of transfersomal vesicles. J Liposome Res. 2012;22(4):336-45.

88. Niu M, Lu Y, Hovgaard L, Wu W. Liposomes containing glycocholate as potential oral insulin delivery systems: preparation, in vitro characterization, and improved protection against enzymatic degradation. Int J Nanomedicine. 2011;6: 1155-66.

89. Chen Y, Lu Y, Chen J, Lai J, Sun J, Hu F, et al. Enhanced bioavailability of the poorly water-soluble drug fenofibrate by using liposomes containing a bile salt. Int J Pharm. 2009;376(1-2):153-60.

90. Niu M, Tan Y, Guan P, Hovgaard L, Lu Y, Qi J, et al. Enhanced oral absorption of insulin-loaded liposomes containing bile salts: a mechanistic study. Int J Pharm. 2014;460(1-2):119-30.

91. Shamma RN, Aburahma MH. Follicular delivery of spironolactone via nanostructured lipid carriers for management of alopecia. Int J Nanomedicine. 2014;9:5449-60.

92. Mohsen AM, Asfour MH, Salama AAA. Improved hepatoprotective activity of silymarin via encapsulation in the novel vesicular nanosystem bilosomes. Drug Dev Ind Pharm. 2017;43(12):2043-54.

93. Feng C, Li X, Dong C, Zhang X, Zhang X, Gao Y. RGD-modified liposomes enhance efficiency of aclacinomycin A delivery: evaluation of their effect in lung cancer. Drug Des Devel Ther. 2015; 9:4613-20.

94. Li H, Liu Y, Zhang Y, Fang D, Xu B, Zhang L, et al. Liposomes as a Novel Ocular Delivery System for Brinzolamide: In Vitro and In Vivo Studies. AAPS PharmSciTech. 2016;17(3):710-7.

95. Sinico C, Valenti D, Manconi M, Lai F, Fadda AM. Cutaneous delivery of 8-methoxypsoralen from liposomal and niosomal carriers. Journal of Drug Delivery Science and Technology. 2006;16(2):115-20.

96. Kawano K, Onose E, Hattori Y, Maitani Y. Higher Liposomal Membrane Fluidity Enhances the in Vitro Antitumor Activity of Folate-Targeted Liposomal Mitoxantrone. Molecular Pharmaceutics. 2009;6(1):98-104.

97. Salem HF, Nafady MM, Ali AA, Khalil NM, Elsisi AA. Evaluation of Metformin Hydrochloride Tailoring Bilosomes as an Effective Transdermal Nanocarrier. Int J Nanomedicine. 2022;17:1185-201.

98. Zafar A, Alruwaili NK, Imam SS, Hadal Alotaibi N, Alharbi KS, Afzal M, et al. Bioactive Apigenin loaded oral nano bilosomes: Formulation optimization to

preclinical assessment. Saudi Pharm J. 2021;29(3):269-79.

99. Gupta Y, Jain A, Jain P, Jain SK. Design and development of folate appended liposomes for enhanced delivery of 5-FU to tumor cells. J Drug Target. 2007;15 (3):231-40.

100. Müller RH, Mäder K, Gohla S. Solid lipid nanoparticles (SLN) for controlled drug delivery – a review of the state of the art. European Journal of Pharmaceutics and Biopharmaceutics. 2000;50(1):161-77.

101. Lim WM, Rajinikanth PS, Mallikarjun C, Kang YB. Formulation and delivery of itraconazole to the brain using a nanolipid carrier system. Int J Nanomedicine. 2014; 9:2117-26.

102. Khalil RM, Abdelbary A, Kocova El-Arini S, Basha M, El-Hashemy HA. Evaluation of bilosomes as nanocarriers for transdermal delivery of tizanidine hydrochloride: in vitro and ex vivo optimization. J Liposome Res. 2019;29(2):171-82.

103. Elsherif NI, Shamma RN, Abdelbary G. Terbinafine Hydrochloride Trans-ungual Delivery via Nanovesicular Systems: In Vitro Characterization and Ex Vivo Evaluation. AAPS PharmSciTech. 2017;18 (2):551-62.

104. Aggarwal A, Jindal P. Modification of crystallization behaviour of sertaconazole by preparing its solid dispersions. Journal of Pharmacy and Allied Health Sciences. 2014;4(1):1.

105. Mokale V, Patil H, Patil A, Shirude P, Naik J, Naik B. Formulation and optimisation of famotidine proniosomes: an in vitro and ex vivo study. Journal of Experimenta Nanoscinece. 2015;11.

106. El-Nabarawi MA, Shamma RN, Farouk F, Nasralla SM. Bilosomes as a novel carrier for the cutaneous delivery for dapsone as a potential treatment of acne: preparation, characterization and in vivo skin deposition assay. J Liposome Res. 2020;30(1):1-11.

107. Shreya AB, Managuli RS, Menon J, Kondapalli L, Hegde AR, Avadhani K, et al. Nano-transfersomal formulations for transdermal delivery of asenapine maleate: in vitro and in vivo performance evaluations. J Liposome Res. 2016;26 (3):221-32.

108. Gaba B, Fazil M, Ali A, Baboota S, Sahni JK, Ali J. Nanostructured lipid (NLCs) carriers as a bioavailability enhancement

tool for oral administration. Drug Delivery. 2015;22(6):691-700.

109. Som I, Bhatia K, Yasir M. Status of surfactants as penetration enhancers in transdermal drug delivery. J Pharm Bioallied Sci. 2012; 4(1):2-9.

110. Muzzalupo R, Tavano L, Cassano R, Trombino S, Ferrarelli T, Picci N. A new approach for the evaluation of niosomes as effective transdermal drug delivery systems. Eur J Pharm Biopharm. 2011;79 (1):28-35.

111. Weng HJ, Tsai TF. ABCB1 in dermatology: roles in skin diseases and their treatment. J Mol Med (Berl). 2021; 99(11):1527-38.

112. Devi M KS, Mahadevan N. Amphotericin-B loaded vesicular systems for the treatment of topical fungal infection. Int J Rec Adv Pharm Res. 2011;4:37–46.

113. Taudorf EH, Jemec GBE, Hay RJ, Saunte DML. Cutaneous candidiasis - an evidence-based review of topical and systemic treatments to inform clinical practice. J Eur Acad Dermatol Venereol. 2019;33(10):1863-73.

114. Rao SH, Bhalekar MR, Kelkar SH, Godbole SS, Kharche RA. Testing the Efficacy of Transungual Drug Delivery System (Nail Lacquer) Containing Terbinafine Against Aspergillus brasiliensis for the Topical Treatment of Onychomycosis. bioRxiv. 2022:2022.02. 03.478980.

115. Manikandan P, Varga J, Kocsubé S, Revathi R, Anita R, Dóczi I, et al. Keratitis caused by the recently described new species Aspergillus brasiliensis: two case reports. Journal of Medical Case Reports. 2010;4(1):68.

116. Murphy A, Kavanagh K. Emergence of Saccharomyces cerevisiae as a human pathogen: Implications for biotechnology. Enzyme and Microbial Technology. 1999; 25(7):551-7.

117. Papadimitriou M, Hatzidaki E, Papasotiriou I. Linearity Comparison of Three Colorimetric Cytotoxicity Assays. Journal of Cancer Therapy. 2019;10(07):580-90.

118. Keepers YP, Pizao PE, Peters GJ, van Ark-Otte J, Winograd B, Pinedo HM. Comparison of the sulforhodamine B protein and tetrazolium

(MTT) assays for in vitro chemosensitivity testing. European Journal of Cancer and Clinical Oncology. 1991;27(7):897-900.

119. Gupta AK, Cooper EA. Update in antifungal therapy of dermatophytosis. Mycopathologia. 2008; 166:353-67.

Peer-review history:
The peer review history for this paper can be accessed here:
https://www.sdiarticle5.com/review-history/118047